

Chiral restoration and deconfinement in two-color QCD with two flavors of staggered quarks

David Scheffler*

Institut für Kernphysik, Technische Universität Darmstadt, 64289 Darmstadt, Germany

E-mail: dscheff@theorie.i kp.physik.tu-darmstadt.de

Christian Schmidt

Fakultät für Physik, Universität Bielefeld, 33501 Bielefeld, Germany

E-mail: schmidt@physik.uni-bielefeld.de

Dominik Smith

Institut für Kernphysik, Technische Universität Darmstadt, 64289 Darmstadt, Germany

E-mail: smith@theorie.i kp.physik.tu-darmstadt.de

Lorenz von Smekal

Institut für Kernphysik, Technische Universität Darmstadt, 64289 Darmstadt, Germany

Institut für Theoretische Physik, Justus-Liebig-Universität, 35392 Gießen, Germany

E-mail: lorenz.smekal@physik.tu-darmstadt.de

In preparation of lattice studies of the two-color QCD phase diagram we study chiral restoration and deconfinement at finite temperature with two flavors of staggered quarks using an RHMC algorithm on GPUs. We first study unquenching effects in local Polyakov loop distributions, and the Polyakov loop potential obtained via Legendre transformation, in a fixed-scale approach for heavier quarks. We also present the chiral condensate and the corresponding susceptibility over the lattice coupling across the chiral transition for lighter quarks. Using Ferrenberg-Swendsen reweighting we extract the maxima of the chiral susceptibility in order to determine pseudo-critical couplings on various lattices suitable for chiral extrapolations. These are then used to fix the relation between coupling and temperature in the chiral limit.

31st International Symposium on Lattice Field Theory LATTICE 2013

July 29 - August 3, 2013

Mainz, Germany

*Speaker.

1. Introduction

Direct calculations using standard Monte-Carlo methods in quantum chromodynamics (QCD) at finite baryon density are hindered by the fermion sign problem. In order to still gain insight into gauge theories at finite densities several theories free of the sign problem have been investigated like two-color QCD [1, 2], adjoint QCD [3, 1] or G_2 -QCD [4, 5]. This work deals with two particular aspects in two-color QCD at finite temperature: the determination of effective Polyakov loop potentials and the study of chiral properties unique to staggered fermions. Here we only present calculations at $\mu = 0$ leaving the inclusion of finite density for upcoming work.

The interest in effective Polyakov loop potentials mainly arises from Polyakov-loop enhanced effective models, like PQM or PNJL models, which use Polyakov loop potentials as an essential input. Little is known about its density dependence, but a good description of the two-color QCD phase diagram seems possible if it were [6]. In contrast to other works where the potential of the volume-averaged Polyakov loop has been studied [7] we here use the local (site-wise) effective potential. In pure gauge this has recently been investigated [8]. We will build on this work by including rather heavy quarks in the staggered formulation in order to assess unquenching effects.

Two-color QCD at vanishing density has a flavor symmetry which is enlarged from the usual $SU(N_f)_L \times SU(N_f)_R \times U(1)_B$ to $SU(2N_f)$ (Pauli-Gürsey symmetry). A chiral condensate or a Dirac mass term break this down to $Sp(N_f)$ in the continuum. In contrast, due to the missing Dirac structure of the staggered discretization, one expects a breaking to $SO(2N_f)$ in the continuum limit for staggered quarks. In our case of $N_f = 2$ the expected breaking pattern in the continuum limit thus is $SU(4) \simeq SO(6) \rightarrow SO(4)$ (whereas for fundamental Dirac fermions in the continuum one would have: $SU(4) \simeq SO(6) \rightarrow Sp(2) \simeq SO(5)$). We are interested in the scaling behavior of this atypical breaking and determine the lattice scale via (pseudo-)critical couplings.

We choose the Wilson gauge action for $SU(2)$ and utilize the standard staggered fermion discretization with the rooting procedure to describe two flavors of quarks in the fundamental representation. Configurations are generated using RHMC.

2. Effective Polyakov loop potentials

Our calculations for evaluating the Polyakov loop effective potential are performed in the fixed scale approach. At fixed values of the coupling β we vary the temporal lattice extent N_t in order to change the temperature according to

$$T(N_t) = \frac{1}{aN_t}. \quad (2.1)$$

Critical couplings, the lattice spacing and the temperature scale for $SU(2)$ have been precisely determined in pure gauge simulations [8]. We employ the same values of the coupling, $\beta_{10} = 2.577856$ and $\beta_{12} = 2.635365$, which are the critical couplings in pure gauge for $N_t = 10$ and 12 lattices. The scale $a\sqrt{\sigma}$ amounts to 0.140 at β_{10} and 0.116 at β_{12} . In our study we use lattices with temporal extent $N_t = 6, 8, 10$ and 12 with an aspect ratio N_s/N_t of 4. Finite volume tests with an aspect ratio of 3 have been performed for some lattices and no difference in observables (average Polyakov loop and chiral condensate) as well as in the local Polyakov loop distributions have been

visible. Relative temperatures have been obtained via

$$\frac{T(N_t)}{T_c} \Big|_{\beta} = \frac{N_t^c}{N_t}. \quad (2.2)$$

The requirement of fixed physical quark masses leads to rescaled quark masses in lattice units at the different values of β :

$$am(\beta') = \frac{a(\beta')}{a(\beta)} \cdot am(\beta) \quad (2.3)$$

Masses have been chosen to be $am = 0.1$ and 0.5 at β_{10} which via Eq. (2.3) results in $am = 0.083$ and 0.414 for β_{12} . Introducing fermions will modify the lattice scale and it would be necessary to determine the scale at the different quark masses. As our quark masses are rather large, we assume that the scale does not change much. At least qualitatively the results should not change.

For the calculation of the local effective Polyakov loop potential we need the Polyakov loop probability distribution $P(l)$. It is obtained via histogramming the Polyakov loop values on the spatial lattice volume and aggregating over the whole ensemble.

From the distribution we first calculate the ‘‘constraint’’ effective potential V_0

$$V_0(l) = -\log P(l). \quad (2.4)$$

Next we perform a Legendre transform as follows:

$$W(h) = \log \int dl \exp(-V_0(l) + hl) \quad V_{\text{eff}}(\hat{l}) = \sup_h (\hat{l}h - W(h)). \quad (2.5)$$

Its minimum is correctly located at the value of the average Polyakov loop.

At the critical temperature T_c the constraint Polyakov loop potential in pure gauge is given by the Vandermonde potential and corresponding distribution

$$V_0^{(T_c)}(l) = -\frac{1}{2} \log(1 - l^2) - C \quad P^{(T_c)}(l) = \frac{2}{\pi} \sqrt{1 - l^2}. \quad (2.6)$$

An ansatz for temperatures above T_c is given by [9]

$$V_0(l) = V_0^{(T_c)}(l) + a(T) - b(T)l + c(T)l^2 \quad (2.7)$$

corresponding to

$$P(l) = \frac{2}{\pi} \sqrt{1 - l^2} \exp(-a(T) + b(T)l - c(T)l^2). \quad (2.8)$$

Figure 1 shows the Polyakov loop distributions for different temperatures comparing pure-gauge results to unquenched ones with two different quark masses. For temperatures at and below the critical temperature in pure gauge the distribution and correspondingly the constraint effective potential (not shown) are perfectly described by Eq. (2.6). $Z(2)$ symmetry is spontaneously broken at temperatures above T_c , leading to an asymmetry towards positive Polyakov loop values in the distribution and the constraint effective potential. The unquenched simulations show a stronger asymmetry in these observables than pure gauge caused by the explicit breaking of the $Z(2)$ symmetry by the finite fermion masses. Explicit symmetry breaking and thus the asymmetry is larger

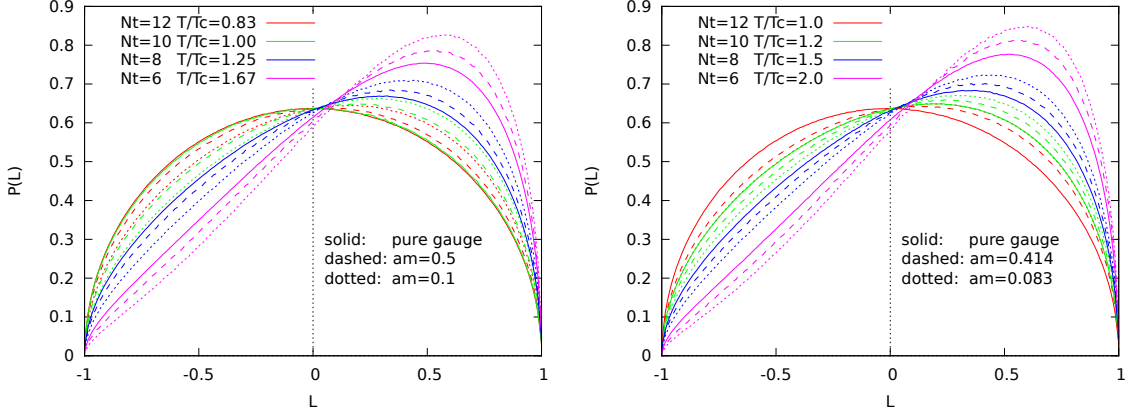


Figure 1: Distribution of the SU(2) Polyakov loop at $\beta = 2.577856$ (left) and $\beta = 2.635365$ (right)

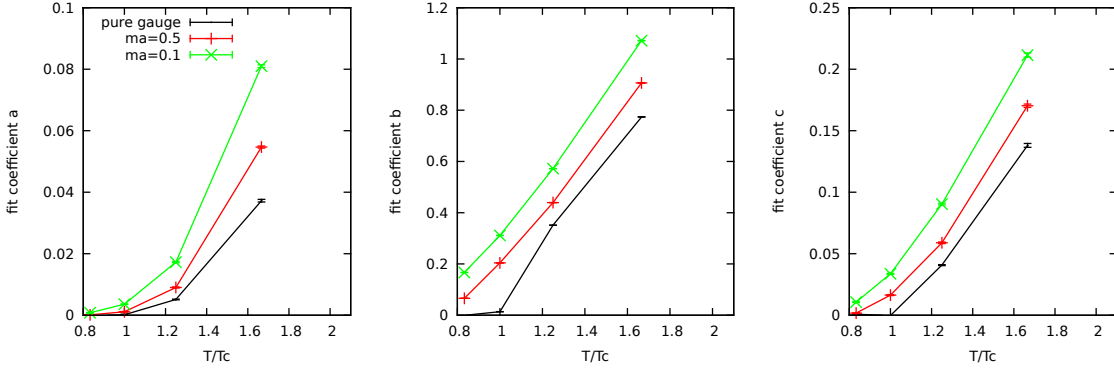


Figure 2: Temperature dependence of fit coefficients for the Polyakov loop distribution at $\beta = 2.577856$

for smaller quark masses. In the effective potentials (not shown) the breaking manifests itself in a shift of the potential minimum towards larger Polyakov loop values.

The temperature-dependent coefficients in Equations (2.7) and (2.8) are obtained from a χ^2 fit. Fig. 2 shows results for $\beta = 2.577856$. We find that all three parameters rise with increasing temperature and also with decreasing mass. Note that $b(T)$ amounts to the breaking of $Z(2)$ center symmetry. This coefficient shows a qualitative difference between the pure gauge results and those with dynamical quarks included: While the coefficient is consistent with zero at and below T_c in the pure gauge case, it no-longer drops to such small values near T_c when dynamical quarks are included due to their explicit symmetry breaking. More details will be reported in [10].

3. Chiral properties

For the analysis of chiral properties we have not used the fixed-scale approach but varied β to change the temperature. The fixed-scale approach is limited by the number of temperature values inside the interesting temperature range. We have performed simulations on various lattice sizes $N_t = 4, 6, 8$ with an aspect ratio $N_s/N_t = 4$, and various fermion masses am between 0.005 and 0.1.

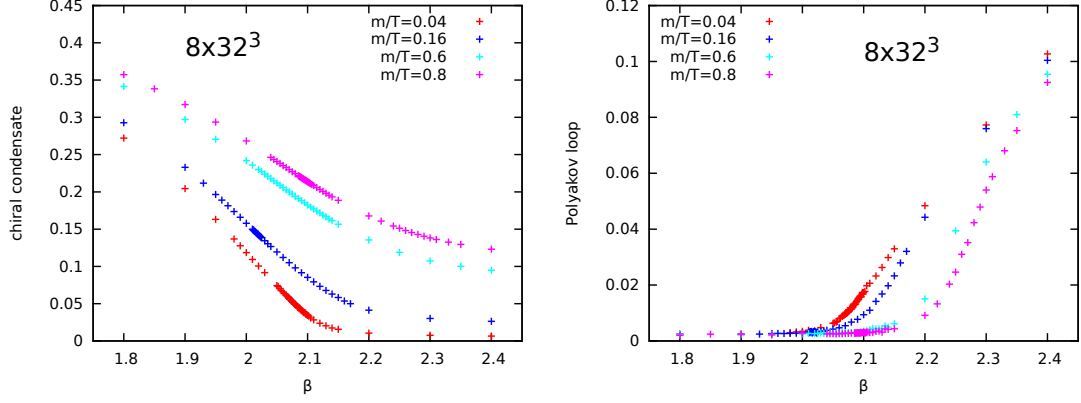


Figure 3: Chiral condensate (left) and Polyakov loop (right) as function of the coupling for different masses

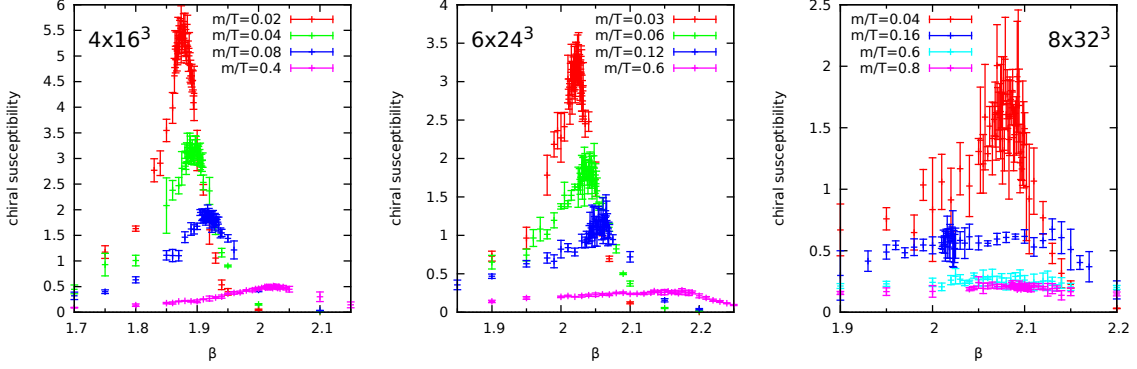


Figure 4: Chiral susceptibility (disconnected part) at different masses and lattice sizes

We first present simple observables, namely the chiral condensate and the Polyakov loop. Figure 3 shows their dependence on the coupling and the quark mass on $N_t = 8$ lattices. Errors are of the size of the symbols or smaller and are omitted for better visibility. We clearly find a crossover transition in both pseudo-order parameters for all masses. For lower quark masses the transition is stronger (steeper) in the chiral condensate and weaker in the Polyakov loop and vice versa which is the expected behavior. The chiral condensate at large couplings is still large for $m/T = 0.6$ and 0.8 due to large explicit symmetry breaking, but drops to low values for $m/T = 0.04$ and 0.16 .

The disconnected part of the chiral susceptibility for several quark masses and lattice sizes is given in Figure 4. For small quark masses clear peaks are visible. Larger sample sizes are needed for most calculations at $N_t = 8$ to reduce statistical errors. From the location of the peaks of the chiral susceptibility we obtain the pseudo-critical couplings as function of temporal lattice extent and quark mass. On lattices with temporal extent of 4 and 6 the peak position can readily be determined. For the $N_t = 4$ results we additionally utilize Ferrenberg-Swendsen reweighting to obtain an even more precise location of the maxima. Unfortunately, on the $N_t = 8$ lattices the peak position is not as clear due to larger statistical uncertainties. In the case of $m/T = 0.8$ and 0.6 we find very broad and flat maxima and thus cannot determine a peak position. Also at $m/T = 0.16$ the uncertainty is so large that we will not include this data point in the determination of the scale.

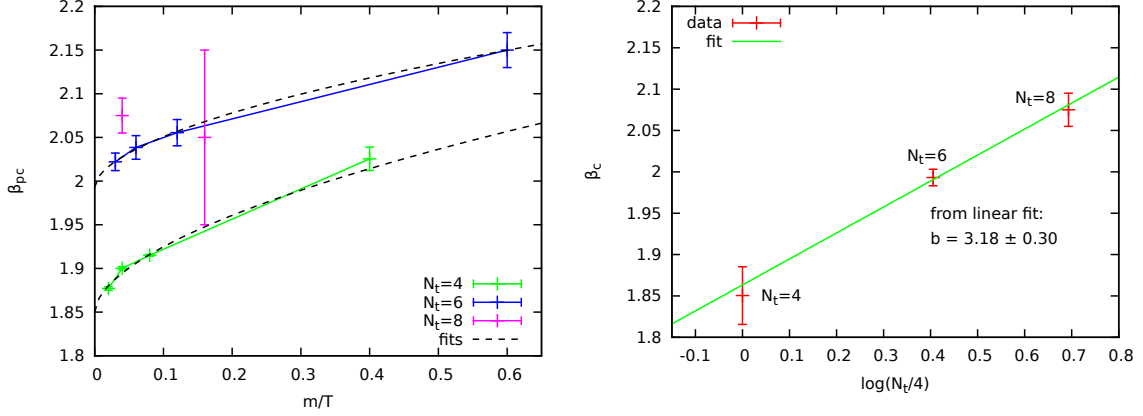


Figure 5: Pseudo-critical couplings (left) and fit for temperature scale (right)

Resulting pseudo-critical couplings are shown in Figure 5 (left). We extrapolate the pseudo-critical couplings to the chiral limit, $m = 0$, separately for $N_t = 4$ and 6 using the ansatz

$$\beta_{pc}(m, N_t) = \beta_c(N_t) + d \cdot (m/T)^c. \quad (3.1)$$

For $N_t = 8$ we use the pseudo-critical coupling of the smallest mass value as our currently best estimate for the critical coupling.

Using these leading scaling behavior fits, we can relate the extrapolated critical couplings for different temporal lattice sizes to a relative temperature scale. At fixed N_t we first assume that we may write, in the chiral limit,

$$\frac{T}{T_c} = \frac{a_c}{a} = \exp\{b(\beta - \beta_c)\}, \quad (3.2)$$

for temperatures T sufficiently close to T_c , where b is a nonperturbative coefficient that we wish to estimate. To do that we compare criticality for different N_t ,

$$1 = \frac{N_t^{(1)} a_c^{(1)}}{N_t^{(2)} a_c^{(2)}} \Leftrightarrow \frac{a_c^{(1)}}{a_c^{(2)}} = \frac{N_t^{(2)}}{N_t^{(1)}} = \exp\{b(\beta_c^{(2)} - \beta_c^{(1)})\}, \quad (3.3)$$

with the same coefficient b (the lattice spacing $a_c^{(2)}$ and coupling $\beta_c^{(2)}$ are not critical on the $N_t^{(1)}$ lattice for which we need their leading logarithmic dependence in (3.2)). From the three different critical couplings at $N_t = 4, 6$ and 8 we obtain $b = 3.18 \pm 0.30$, compare Figure 5 (right). For comparison, from the deconfinement phase transition in the pure gauge theory the corresponding value has incidently been determined to be $b = 3.28 \pm 0.07$ [8].

Close to criticality we furthermore expect magnetic scaling. The exponent c in our fit ansatz (3.1) for example, with (3.2) at leading order in the critical temperature $t = T/T_c - 1$ determines the variation of the location $t_{\max}(m) \sim m^{1/(\beta\delta)}$ of the susceptibility maxima with the explicitly symmetry breaking m [11], hence $c^{-1} = \beta\delta$. A global fit to our $N_t = 4$ and 6 data yields $c = 0.6(2)$ as our currently best estimate for the expected $SO(6) \rightarrow SO(4)$ universality class.

In order to determine the critical exponents β and δ , and with two exponent-scaling the remaining ones from scaling and hyperscaling relations as well, we need a second estimate, however.

One candidate is the height $\chi_{\max}(m)$ of the peak in the chiral susceptibility, whose leading behavior as function of the quark mass around criticality is given by

$$\chi_{\max}(m)/T^2 = \chi(m)|_{\beta_{pc}(N_t, m)}/T^2 \sim (m/T_c)^{1/\delta-1}. \quad (3.4)$$

Another possibility is to investigate the mass dependence of the chiral condensate right at the critical coupling,

$$m \langle \bar{\psi}\psi \rangle(m)|_{\beta_c(N_t)}/T_c^4 \sim (m/T_c)^{1/\delta+1}, \quad (3.5)$$

Both are governed by the same critical exponent δ . Unfortunately, the accuracy of our present determinations of the susceptibility maxima is not yet sufficient to obtain consistent results. From our currently best analysis with Ferrenberg-Swendsen reweighting of the $N_t = 4$ lattice data, at the moment we obtain $\delta = 3.4(3)$ with Eq. (3.4) as compared to $\delta = 4.25(3)$ from Eq. (3.5).

4. Summary and outlook

We have assessed the unquenching effects of quarks on the effective Polyakov loop potential. Regarding the chiral sector we have started the determination of a relative scale. Further simulations at $\mu = 0$ are ongoing to improve this determination. They will hopefully allow us to also obtain more reliable results for the critical exponents eventually. After analyzing two-color QCD along the temperature axis at $\mu = 0$ we will proceed to finite chemical potential and investigate the influence of finite density on the effective Polyakov loop potential for a start.

Acknowledgements

This work was supported by the BMBF under contract 06DA9047I, by the Deutsche Forschungsgemeinschaft within SFB 634, by the Helmholtz International Center for FAIR within the LOEWE initiative of the State of Hesse and by the European Commission, FP7-PEOPLE-2009-RG, No. 249203.

References

- [1] S. Hands, I. Montvay, S. Morrison, M. Oevers, L. Scorzato, *et al.* *Eur.Phys.J.* **C17** (2000) 285–302.
- [2] S. Cotter, P. Giudice, S. Hands, and J.-I. Skullerud *Phys.Rev.* **D87** (2013) 034507.
- [3] F. Karsch and M. Lütgemeier *Nucl.Phys.* **B550** (1999) 449–464.
- [4] A. Maas, L. von Smekal, B. Wellegehausen, and A. Wipf *Phys.Rev.* **D86** (2012) 111901.
- [5] L. von Smekal, B. H. Wellegehausen, A. Maas, and A. Wipf [arXiv:1310.7745](#) [hep-lat].
- [6] N. Strodthoff and L. von Smekal [arXiv:1306.2897](#) [hep-ph].
- [7] C. S. Fischer, L. Fister, J. Lücker, and J. M. Pawłowski [arXiv:1306.6022](#) [hep-ph].
- [8] D. Smith, A. Dumitru, R. Pisarski, and L. von Smekal *Phys. Rev.* **D88** (2013) 054020.
- [9] D. Smith *Phys. Rev.* **D82** (2010) 034503.
- [10] D. Scheffler, P. Scior, D. Smith, L. von Smekal, and B. H. Wellegehausen in preparation.
- [11] A. Pelissetto and E. Vicari *Phys.Rept.* **368** (2002) 549–727.